

FORMATION OF THE FIRST STARS AND QUASARS

Z. Haiman^{1,2}

¹*Astronomy Department, Harvard University, 60 Garden Street, Cambridge, MA 02138, USA*

²*NASA/Fermilab Astrophysics Center, Fermi National Accelerator Laboratory, P.O. Box 500, Batavia, IL 60510, USA*

ABSTRACT

We examine various observable signatures of the first generation of stars and low-luminosity quasars, including the metal enrichment, radiation background, and dust opacity/emission that they produce. We calculate the formation history of collapsed baryonic halos, based on an extension of the Press–Schechter formalism, incorporating the effects of pressure and H₂–dissociation. We then use the observed C/H ratio at $z=3$ in the Lyman– α forest clouds to obtain an average the star formation efficiency in these halos. Similarly, we fit the efficiency of black-hole formation, and the shape of quasar light curves, to match the observed quasar luminosity function (LF) between $z=2$ –4, and use this fit to extrapolate the quasar LF to faint magnitudes and high redshifts. To be consistent with the lack of faint point–sources in the Hubble Deep Field, we impose a lower limit of ~ 75 km s^{−1} for the circular velocities of halos harboring central black holes.

We find that in a Λ CDM model, stars reionize the IGM at $z_{\text{reion}}=9$ –13, and quasars at $z=12$. Observationally, z_{reion} can be measured by the forthcoming MAP and Planck Surveyor satellites, via the damping of CMB anisotropies by $\sim 10\%$ on small angular scales due to electron scattering. We show that if reionization occurs later, at $5 \lesssim z_{\text{reion}} \lesssim 10$, then it can be measured from the spectra of individual sources. We also find that the Next Generation Space Telescope will be able to directly image about 1–40 star clusters, and a few faint quasars, from $z > 10$ per square arcminute. The amount of dust produced by the first supernovae has an optical depth of $\tau=0.1$ –1 towards high redshift sources, and the reprocessed UV flux of stars and quasars distorts the cosmic microwave background radiation (CMB) by a Compton y -parameter comparable to the COBE limit, $y \sim 1.5 \times 10^{-5}$.

INTRODUCTION

One of the outstanding problems in cosmology is the nature of the first generation of astrophysical objects which appeared when the universe first transformed from its initial smooth state to its current clumpy state. Although we have observational data on bright quasars and galaxies out to redshifts $z \sim 5$ and on the linear density fluctuations at redshift $z \sim 10^3$, there is currently no direct evidence as to when and how the first structures formed, and what kind of objects were responsible for the end of the “dark age” of the universe (Rees 1996).

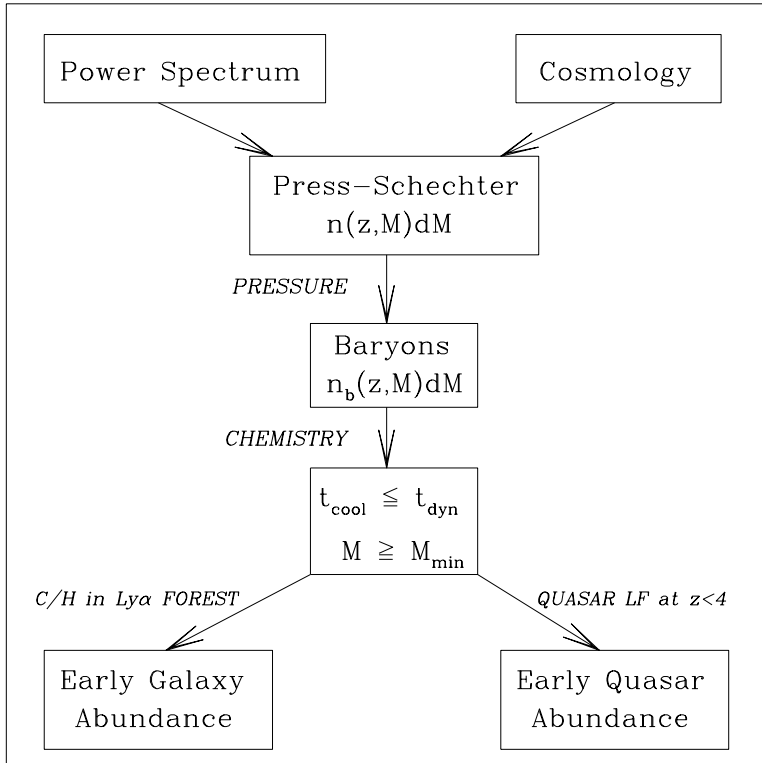


Fig. 1: *Schematic View of Extrapolations to $z > 5$.*

Popular Cold Dark Matter (CDM) models for structure formation predict the appearance of the first baryonic objects with masses $M \sim 10^5 M_\odot$ at redshifts as high as $z \sim 30$; objects with progressively higher masses assemble later. Following virialization, the gas in these objects can only continue to collapse and fragment if it can cool on a timescale shorter than the Hubble time. In the metal-poor primordial gas, the only coolants that satisfy this requirement are neutral atomic hydrogen (H) and molecular hydrogen (H_2). However, H_2 molecules are fragile, and are easily photodissociated throughout the universe by trace amounts of starlight (Haiman, Rees, & Loeb 1997). Hence, most of the first stars are expected to form inside objects with virial temperatures $T_{\text{vir}} \gtrsim 10^4 \text{ K}$. Depending on the details of their cooling and angular momentum transport, the gas in these objects is expected to either fragment into stars, or form a central black hole exhibiting quasar activity. Conversion of a small fraction ($\sim 1 - 10\%$) of the gas into stars or quasars could reionize the universe, and strongly affect the entropy of the intergalactic medium.

Here, we explore the impact of early stars and quasars on the reionization history of the universe, as well as their effects on the CMB. For both types of sources, we calibrate the total amount of light they produce based on data from redshifts $z \lesssim 5$. The efficiency of early star formation is calibrated based on the observed metallicity of the intergalactic medium (Tytler et al. 1995, Songaila & Cowie 1996), while the early quasars are constrained to match the quasar luminosity function at redshifts $z \lesssim 5$ (Pei 1995), as well as data from the Hubble Deep Field (HDF) on faint point-sources. We focus on a particular cosmological model with a cosmological constant, namely the “concordance model” of Ostriker & Steinhardt (1995). Within this model, we predict the number of high-redshift star-clusters, and low-luminosity quasars, using

the Press–Schechter formalism (Press & Schechter 1974). For results in other cosmological models, as well as a more detailed description of our methods and results, we refer the reader to several papers (Haiman, Rees & Loeb 1997; Haiman & Loeb 1997a,b; Loeb & Haiman 1997; Haiman & Loeb 1998a,b; and Haiman, Madau & Loeb 1998).

MODELING METHOD

The method described below is based on the Press–Schechter formalism, and is depicted schematically in Figure 1. The most important aspects of our modeling are the inclusion of gas pressure, introducing the requirement of efficient cooling, and calibrating the formation rate of stars or black holes to the halo formation rate, using observational data available at $z < 5$.

Formation of Dark Halos

The change in the comoving number density of dark halos with masses between M and $M + dM$, between redshifts z and $z + dz$, is governed by the derivative,

$$\frac{d^2N(M, z)}{dM dz} = \frac{d}{dz} \frac{dN_{\text{ps}}(M, z)}{dM} \quad (1)$$

where $dN_{\text{ps}}/dM(M, z)$ is the Press–Schechter mass function. The actual halo formation rate is larger than the derivative $\frac{d}{dz}(dN_{\text{ps}}/dM)$, since this derivative includes a negative contribution from merging halos. However, at high redshifts collapsed objects are rare, and the merger probability is low. We have compared the above expression with the more accurate result for the halo formation rate given by Sasaki (1994), and confirmed that the difference in the rates is negligible for the high redshifts and halo masses under consideration here. We therefore use Eq. (1) to describe the dark halo formation rate at high redshifts.

Effects of Gas Pressure

Although we use the Press–Schechter mass–function to find the abundance and mass distribution of dark matter halos, this does not directly yield the corresponding mass–function of baryonic clouds. Initially, most of the collapsed baryons are in low–mass systems near the Jeans mass, and therefore the pressure of the baryons has a significant effect on the overall collapsed fraction. Effectively, the collapse of the baryons within each halo is delayed relative to the dark matter (Haiman, Thoul & Loeb 1996), reducing the baryon fraction of low–mass halos below the initial Ω_b . We obtained the exact collapse redshifts, and baryon fractions, of spherically symmetric perturbations by following the motion of both the baryonic and the dark matter shells with a one dimensional hydrodynamics code (Haiman & Loeb 1997a). This produces a one–to–one mapping of dark matter mass to baryon mass within each halo, as a function of halo mass and collapse redshift, which we then use to obtain $d^2N_b/dM_b dz$, the rate of change of mass function of gas clouds, as a function of cloud mass and redshift.

Effect of Cooling

Following collapse and virialization, the gas within each cloud can only continue to collapse if it can cool on a timescale shorter than the Hubble time. This is a necessary condition for a cloud to form either stars or central black holes, and translates to a lower limit on the cloud temperature, or the cloud mass. In the metal–poor primordial gas, there are two cooling agents that satisfy this requirement: neutral atomic hydrogen (H) and molecular hydrogen (H_2); the former is effective at $T_H \gtrsim 10^4 \text{ K}$, the latter at $T_{H_2} \gtrsim 10^2 \text{ K}$. Taking the temperature of each collapsed gas cloud to be the virial temperature, these limits would imply the low mass cutoffs of $M_H \sim 10^8 M_\odot [(1 + z_{\text{vir}})/10]^{-3/2}$ or $M_{H_2} \sim 10^5 M_\odot [(1 + z_{\text{vir}})/10]^{-3/2}$, respectively.

Since we found that H_2 molecules are fragile, and are easily photodissociated throughout the universe by trace amounts of starlight (Haiman, Rees, & Loeb 1997), we here assume that most of the first stars or quasars are formed via atomic H cooling, inside objects with masses $M \gtrsim M_{\text{H}}$.

Star-Formation Efficiency

One possible fate of each collapsed gas cloud that can cool and continue to collapse is to fragment into stars. We here ignore the actual fragmentation process, and simply calibrate the fraction f_{star} of the collapsed gas that must have been converted into stars, by requiring it to reproduce the universal average C/H ratio, inferred from CIV absorption lines in Ly α forest clouds. We assume that the carbon produced in the early star clusters is homogeneously mixed with the rest of the baryons; incomplete mixing would necessitate more stars than we derive. The C/H ratio deduced from the observations is between 10^{-3} and 10^{-2} of the solar value (Songaila 1997). We use tabulated ^{12}C yields of stars with various masses, and consider three different initial mass functions (IMFs). The uncertainty in the total carbon production is a factor of ~ 10 ; a factor of ~ 3 is from the uncertainty in the carbon yields of $3 - 8M_{\odot}$ stars due to the unknown extent of hot bottom burning (Renzini & Voli 1981), and another factor of ~ 3 is due to the difference between the Scalo and Miller-Scalo (1979) IMFs. To be conservative, we assume inefficient hot bottom burning, i.e. maximum carbon yields. Under these assumptions, we find that the condition $10^{-3}[\text{C}/\text{H}]_{\odot} < \text{C}/\text{H} < 10^{-2}[\text{C}/\text{H}]_{\odot}$ translates into $1.7\% < f_{\text{star}} < 17\%$. Since the collapsed fraction at $z = 3$ is $\sim 50\%$, the fraction of all baryons in stars is $\sim 0.8\text{--}8\%$. A factor of ~ 3 is included in this number due to the finite time required to produce carbon inside the stars; i.e. only a third of the total stellar carbon is produced and ejected by $z = 3$.

Black-Hole Formation Efficiency and Quasar Light-Curve

Another possible fate of a gas cloud that can cool is to continue collapsing, and to form a central black hole, exhibiting quasar-like activity. To quantify this scenario, here we assume that the luminosity history of each black hole depends only on its mass, and postulate the existence of a universal quasar light-curve in Eddington units. This approach is motivated by the fact that for a sufficiently high fueling rate, quasars are likely to shine at their maximum possible luminosity, which is some constant fraction of the Eddington limit, for a time which is dictated by their final mass and radiative efficiency. We also assume that the final black hole mass is a fixed fraction of the total halo mass, and allow this fraction to be a free parameter. Based on this minimal set of assumptions, we demonstrated that there exists a universal light curve [$f(t) = (L_{\text{Edd}}/M_{\text{bh}}) \exp(-t/t_0)$, with $t_0 = 10^{5.82}$], for which the Press-Schechter theory provides an excellent fit to the observed evolution of the luminosity function of bright quasars between redshifts $2.6 < z < 4.5$. Furthermore, our fitting procedure results in a black hole to halo mass ratio of $M_{\text{bh}}/M_{\text{gas}} = 10^{-3.2}\Omega_{\text{m}}/\Omega_{\text{b}} = 5.4 \times 10^{-3}$, close to the typical value $\sim 6 \times 10^{-3}$ found in local galaxies (Kormendy *et al.* 1997; Magorrian *et al.* 1998). Given this ratio and the fitted light-curve, we then extrapolate the observed LF to higher redshifts and low luminosities. Note, however, that our solution is not unique, and with the introduction of additional free parameters, a non-linear (mass and redshift dependent) black-hole mass to halo mass relation can also lead to acceptable fits to the observed quasar LF (Haehnelt, Natarajan, & Rees 1998). The actual formation process of low-luminosity quasars was addressed in detail by Eisenstein & Loeb (1995), and Loeb (1997).

Constraints from the Hubble Deep Field

High resolution, deep imaging surveys can be used to set important constraints on semi-analytical structure formation models. We have found that the lack of unresolved B-band “dropouts” with $V > 25$ mag in the

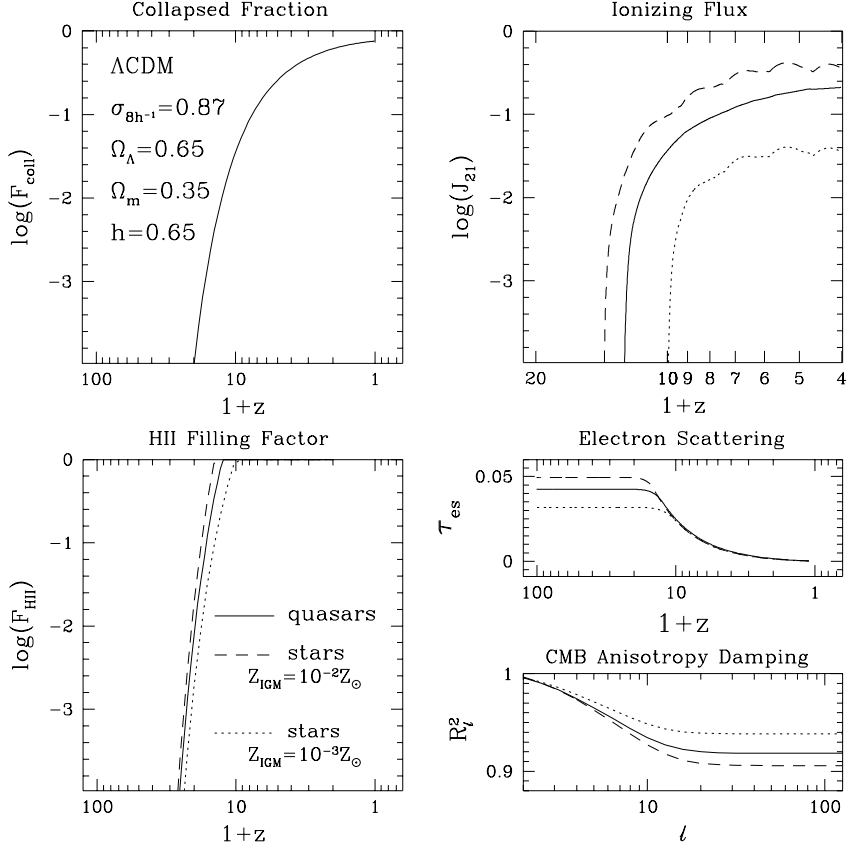


Fig. 2: *Reionization History.* Clockwise, the different panels show: (i) the collapsed fraction of baryons; (ii) the background flux at the Lyman edge; (iii) the volume filling factor of ionized hydrogen; and (iv) the optical depth to electron scattering, and the corresponding damping factor for the power-spectrum decomposition of microwave anisotropies as a function of the spherical harmonic index l . The solid curves refer to quasars, while the dotted/dashed curves correspond to stars with low/high normalization for the star formation efficiency (Haiman & Loeb 1998a).

Hubble Deep Field (HDF) appears to be inconsistent with the expected number of quasars if massive black holes form with a constant universal efficiency in all CDM halos, extending down to halos with virial temperatures of $T_{\text{vir}} = 10^4 \text{ K}$ as outlined above. To reconcile the models with the data, a mechanism is needed that suppresses the formation of quasars in halos with circular velocities $v_{\text{circ}} \lesssim 50 - 75 \text{ km s}^{-1}$. This feedback naturally arises due to the photoionization heating of the gas by the UV background. We have considered several alternative effects that would help reduce the quasar number counts, and find that these can not alone account for the observed lack of detections (Haiman, Madau & Loeb 1998). We therefore impose a lower cutoff of $\sim 75 \text{ km s}^{-1}$ for the circular velocities of halos harboring central black holes.

RESULTS

Reionization

Given the star-formation or quasar black-hole formation histories obtained above, we derive the reionization history of the IGM by following the radius of the expanding Strömgren sphere around each source.

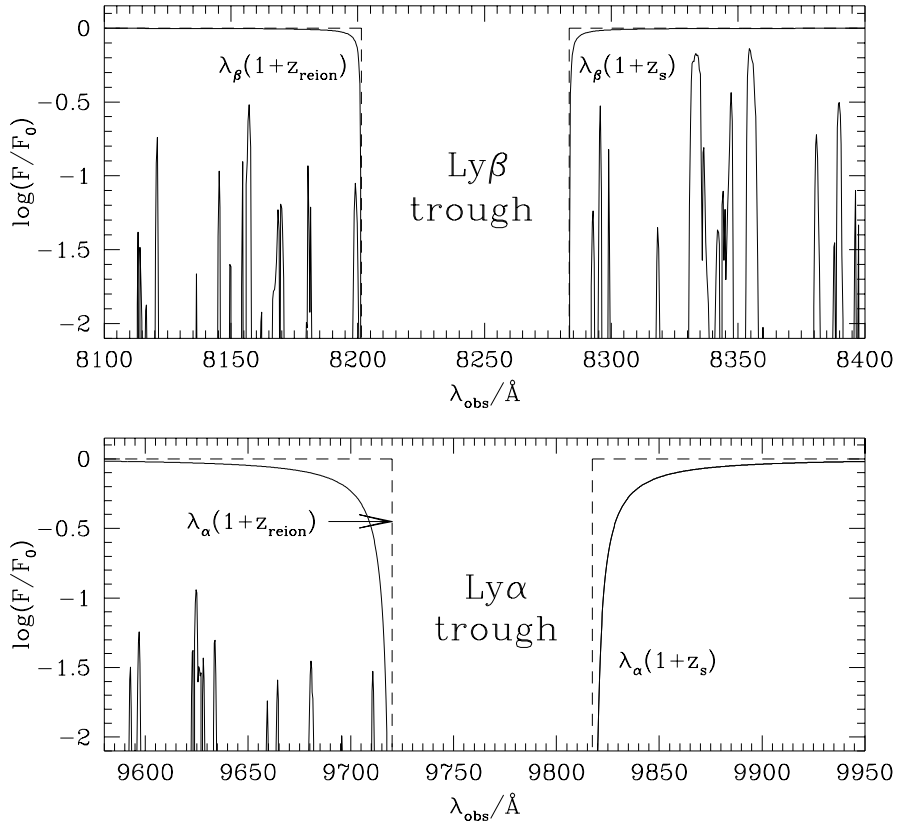


Fig. 3: Spectrum of a source at $z_s = 7.08$, assuming sudden reionization at a redshift $z_{\text{reion}} = 7$. The solid curves show the spectrum without absorption by the high-redshift Ly α forest, and the dashed lines show the spectrum when the damping wings are also ignored.

The reionization history depends on the time-dependent production rate of ionizing photons, their escape fraction, and the number of recombinations in the IGM, which are all functions of redshift. The ionizing photon rate per quasar follows from a median quasar spectrum (Elvis et al. 1994) and the light-curve we derived. The analogous rate per star follows from a time-dependent composite stellar spectrum, constructed from standard stellar atmosphere atlases (Kurucz 1993) and evolutionary tracks (Schaller et al 1992). We also included the feedback from the fact that the collapse of new clouds is suppressed in regions that are already ionized.

Figure 2 summarizes the resulting reionization histories of stars or quasars (solid lines) in our Λ CDM cosmology. The results for stars are shown in two cases, one with $Z_{\text{IGM}} = 10^{-2} Z_{\odot}$ (dashed lines) and the other with $Z_{\text{IGM}} = 10^{-3} Z_{\odot}$ (dotted lines), to bracket the allowed IGM metallicity range. The panels in Figure 2 show (clockwise) the collapsed fraction of baryons; the evolution of the average flux, J_{21} at the local Lyman limit frequency, in units of $10^{-21} \text{ erg s}^{-1} \text{ cm}^{-2} \text{ Hz}^{-1} \text{ sr}^{-1}$, the resulting evolution of the ionized fraction of hydrogen, F_{HII} , and the consequent damping of the CMB anisotropies. The dashed and dotted curves indicate that stars ionize the IGM by a redshift $9 \lesssim z \lesssim 13$; while the solid curve shows that quasars reionize the IGM at $z = 11.5$. This result can be understood in terms of the total number of ionizing photons produced per unit halo mass: the relative ratios of this number in the three cases are $1 \div 0.37 \div 0.1$, respectively. It is interesting to note, given our quasar and stellar template spectra, that stars will not reionize HeII, while quasars reionize HeII at slightly above the H reionization redshift.

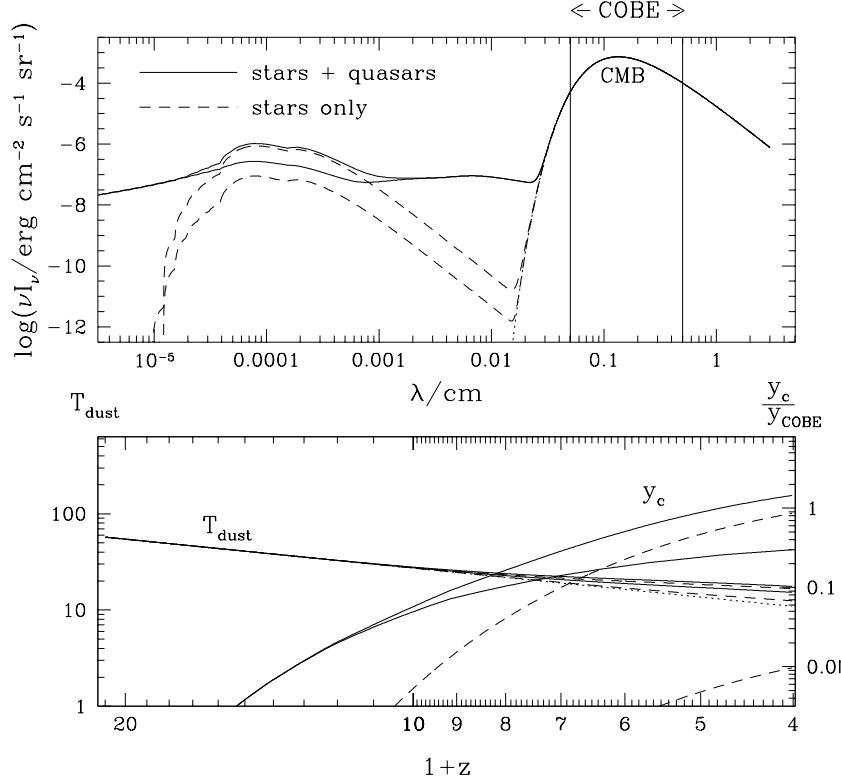


Fig. 4: *Effect of Dust on the Background Flux.*

In these scenarios the reionization redshift z_{reion} can be inferred from the observations of the CMB (see next section). However this method relies on post-reionization electron scattering, which has a detectable optical depth only if $z_{\text{reion}} \gtrsim 10$. It is therefore interesting to ask how z_{reion} can be measured in general. In particular, for $z_{\text{reion}} \lesssim 10$ this would be possible from the spectra of individual high-redshift sources. The spectrum of a source at a redshift $z_s > z_{\text{reion}}$ should show a Gunn–Peterson (GP, 1965) trough due to absorption by the neutral IGM at wavelengths shorter than the local Ly α resonance at the source, $\lambda_{\text{obs}} < \lambda_{\alpha}(1 + z_s)$. By itself, the detection of such a trough would not uniquely establish the fact that the source is located beyond z_{reion} , since the lack of any observed flux could be equally caused by (i) ionized regions with some residual neutral fraction, (ii) individual damped Ly α absorbers, or (iii) line blanketing from lower column density Ly α forest absorbers. On the other hand, for a source located at a redshift z_s beyond but close to reionization, $(1 + z_{\text{reion}}) < (1 + z_s) < \frac{32}{27}(1 + z_{\text{reion}})$, the GP trough splits into disjoint Lyman α , β , and possibly higher Lyman series troughs, with some transmitted flux in between these troughs. Although the transmitted flux is suppressed considerably by the dense Ly α forest after reionization, it is still detectable for sufficiently bright sources and can be used to infer the reionization redshift.

As an example, we show in Figure 3 the simulated spectrum around the Ly α and β GP troughs of a source at redshift $z_s = 7.08$, assuming reionization occurs suddenly at $z_{\text{reion}} = 7$. We have included the effects of a mock catalog of Ly α absorbers along the lines of sight, whose statistics were chosen to obey the observational data at $z < 4.3$ (Press & Rybicki 1993). Although the continuum flux is strongly suppressed, the spectrum contains numerous transmission features; these features are typically a few Å wide, have a central intensity of a few percent of the underlying continuum, and are separated by ~ 10 Å. With a

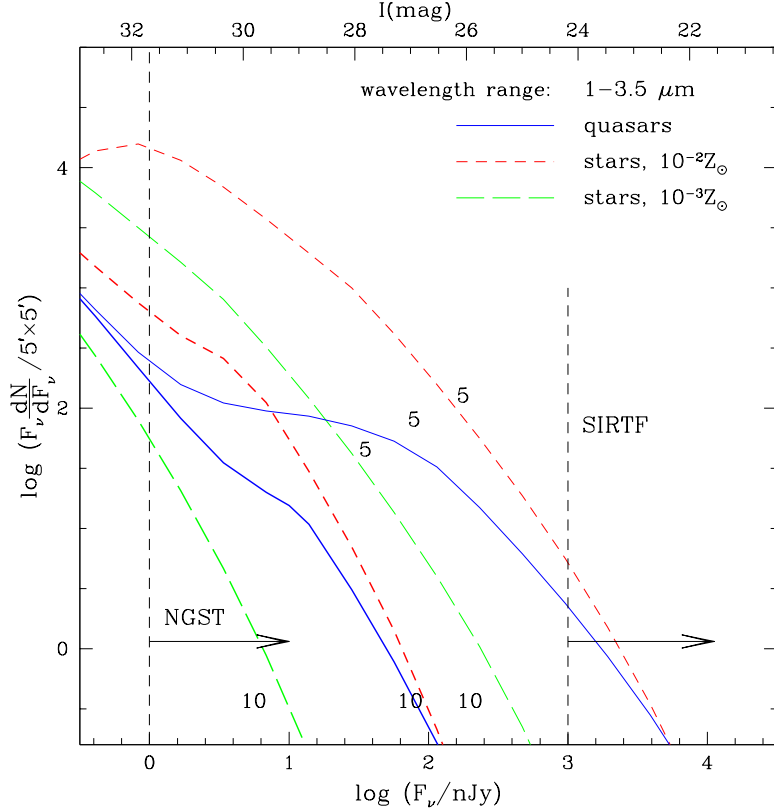


Fig. 5: *Infrared Number Counts.* The solid curves refer to quasars, while the long(short) dashed curves correspond to star clusters with low(high) normalization for the star formation efficiency. The curves labeled “5(10)” show the cumulative number of objects with redshifts above $z = 5(10)$ (Haiman & Loeb 1998a).

sensitivity reaching 1% of the continuum, the blue edges of the GP troughs could be identified to a ~ 10 Å accuracy, leading to a measurement of z_{reion} to a $\sim 10/8200 \sim 0.1\%$ precision. Note that this accuracy is similar to the level allowed by peculiar velocities of a few hundred km/s, which could move either observed edge of the GP trough by ~ 10 Å. Based on Figure 5 below, we expect that the Next Generation Space Telescope would reach the spectroscopic sensitivity required for the detection of sources suitable for this type of measurement (see Haiman & Loeb 1998b for details).

Signatures Imprinted on the Cosmic Microwave Background

Reionization results in a reduction of the temperature anisotropies of the CMB, due to Thomson scattering between the free electrons and CMB photons. Given the ionized fraction of hydrogen as a function of redshift, the electron scattering optical depth (τ_{es}), as well as the multiplicative anisotropy damping factor (R_ℓ^2), as a function of the spherical harmonic index ℓ , can be readily obtained (Hu & White 1997). As shown in the lower right panel of Figure 2, the amplitude of the anisotropies is reduced by an amount between 6–10% on small angular scales (large ℓ). Although small, this reduction is within the proposed sensitivities of the future MAP and Planck satellite experiments, provided data on both temperature and polarization anisotropies of the CMB is gathered (see Table 2 in Zaldarriaga *et al.* 1997).

The stellar dust inevitably produced by the first type II supernovae absorbs the UV emission from early stars and quasars, re-emits it at longer wavelengths, and distorts the CMB spectrum. We calculated

this spectral distortion assuming that each type II supernova yields $0.3M_{\odot}$ of dust with the wavelength-dependent opacity of Galactic dust (Mathis 1990), which gets uniformly distributed within the intergalactic medium. The top panel of Figure 4 shows the resulting total spectrum of the radiation background (CMB + direct stellar and quasar emission + dust emission) at $z = 3$ (more distortion could be added between $0 < z < 3$ by dust and radiation from galaxies). The deviation from the pure $2.728(1+z)$ K blackbody shape is quantified by the Compton y -parameter, whose redshift evolution is shown in the bottom panel. Ignoring the UV flux from quasars, we obtain $1.3 \times 10^{-7} < y_c < 1.2 \times 10^{-5}$ at $z = 3$ (dashed lines), just below the upper limit set by COBE, $y = 1.5 \times 10^{-5}$ (Fixsen et al. 1996). Adding the UV flux of quasars increases the y -parameter to $4.1 \times 10^{-6} < y_c < 2.0 \times 10^{-5}$. It is interesting to note a substantial fraction ($\sim 17\text{--}82\%$) of this y -parameter results simply from the direct far-infrared flux of early quasars, and should be present even in the absence of any intergalactic dust.

Infrared Number Counts

Finally, we examine the feasibility of direct detection of the early population of star clusters, and quasars, motivated by the Next Generation Space Telescope (*NGST*). *NGST* is scheduled for launch in 2007, and is expected to reach a sensitivity of ~ 1 nJy for imaging in the wavelength range $1\text{--}3.5\mu\text{m}$ (Mather & Stockman 1996). Figure 5 shows the predicted number counts, normalized to a $5' \times 5'$ field of view. This figure shows separately the number per logarithmic flux interval of all objects with $z > 5$ (thin lines), and with $z > 10$ (thick lines). The number of detectable sources is high: *NGST* will be able to probe about ~ 100 quasars at $z > 10$, and ~ 200 quasars at $z > 5$ per field of view. The bright-end tail of the number counts approximately follows the power law $dN/dF_{\nu} \propto F_{\nu}^{-2.5}$. The dashed lines show the corresponding number counts of “star-clusters”, i.e. assuming that each halo shines due to a starburst that converts a fraction 0.017-0.17 of the gas into stars. These indicate that *NGST* would detect $\sim 40\text{--}300$ star-clusters at $z > 10$ per field of view, and $\sim 600\text{--}10^4$ clusters at $z > 5$. Unlike quasars, star clusters could in principle be resolved, if they extend over a scale comparable to the virial radius of the collapsed halo (Haiman & Loeb 1997b).

CONCLUSIONS

Based on a combination of cosmological models with simple phenomenological prescriptions for high-redshift star and quasar black hole formation, we find that early stars and quasars would reionize the IGM at high enough redshifts to be observable by the MAP and Planck satellites via the corresponding reduction of the CMB anisotropies. If the reionization redshift is lower, than it can be inferred from the spectra of individual high-redshift sources. The Compton y -parameter for the spectral distortion of the CMB due to early stellar dust is just below the existing COBE upper limit. Most directly, a typical image by *NGST* might reveal numerous early star clusters and quasars.

ACKNOWLEDGEMENTS

I would like to thank my former advisor, Avi Loeb, for years of advice and encouragement, and Anne Kinney for the opportunity to present my work at the COSPAR assembly.

REFERENCES

Eisenstein, D. J., and Loeb, A., *Astrophys. J.*, **443**, 11 (1995).
 Elvis, M., Wilkes, B. J., McDowell, J. C., Green, R. F., Bechtold, J., Willner, S. P., Oey, M. S., Polomski, E., and Cutri, R., *Astrophys. J. Suppl.*, **95**, 1 (1994).

Fixsen, D. J., Cheng, E. S., Gales, J. M., Mather, J. C., Shafer, R. A., and Wright, E. L., *Astrophys. J.*, **473**, 576 (1996).

Gunn, J. E., & Peterson, B. A., *Astrophys. J.*, **142**, 1633 (1965).

Haehnelt, M. G., Natarajan, P., and Rees, M. J., preprint astro-ph/9712259 (1997).

Haehnelt, M. G., and Rees, M. J.: 1993, *Mon. Not. R. Astr. Soc.*, **263**, 168 (1993).

Haiman, Z., and Loeb, A., *Astrophys. J.*, **483**, 21 (1997a)

Haiman, Z., and Loeb, A., in *Proceedings of Science with the Next Generation Space Telescope*, eds. E. Smith and A. Koratkar (1997b).

Haiman, Z., and Loeb, A., *Astrophys. J.*, **503**, 505 (1998a).

Haiman, Z., and Loeb, A., *Astroph. J.*, submitted, preprint astro-ph/9807070 (1998b).

Haiman, Z., Madau, P., and Loeb, A., *Astroph. J.*, in press, preprint astro-ph/9805258 (1998).

Haiman, Z., Rees, M. J. R., and Loeb, A., *Astrophys. J.*, **476**, 458 (1997).

Haiman, Z., Thoul, A., and Loeb, A., *Astrophys. J.*, **464**, 523 (1996).

Hu, W., and White, M., *Astrophys. J.*, **479**, 568 (1997).

Kormendy, J., Bender, R., Magorrian, J., Tremaine, S., Gebhardt, K., Richstone, D., Dressler, A., Faber, S. M., Grillmair, C., and Lauer, T. R., *Astrophys. J. Lett.*, **482**, L139 (1997).

Kurucz, R., CD-ROM No. 13, ATLAS9 Stellar Atmosphere Programs (1993).

Loeb, A., in *Proceedings of Science with the Next Generation Space Telescope*, eds. E. Smith and A. Koratkar (1997b).

Loeb, A., and Haiman, Z., *Astrophys. J.*, **490**, 571 (1997).

Magorrian, J., *et al.*, \AA 115 2285 (1998).

Mather J & Stockman, P., *STSci Newsletter* **13**, 15 (1996).

Mathis, J. S., *Ann. Rev. Astron. Astrophys.*, **28**, 37 (1990).

Miller, G. E., and Scalo, J. M., *Astrophys. J. Suppl.*, **41**, 513 (1979).

Ostriker, J. P., and Steinhardt, P. J., *Nature*, **377**, 600 (1995).

Pei, Y. C., *Astrophys. J.*, **438**, 623 (1995).

Press, W. H., and Rybicki, G. B., *Astrophys. J.*, **418**, 585 (1993).

Press, W. H., and Schechter, P. L., *Astrophys. J.*, **181**, 425 (1974).

Rees, M. J., preprint astro-ph/9608196 (1996).

Renzini, A., and Voli, M., \AA 94 175 (1981).

Sasaki, S., *Publ. Astron. Soc. Japan*, **46**, 427 (1994).

Scalo, J. M., *Fund. Cosm. Phys.*, **11**, 1 (1986).

Schaller, G., Schaefer, D., Meynet, G., and Maeder, A., *Astron. Astrophys. Suppl. Ser.*, **96**, 269 (1992).

Songaila, A., *Astrophys. J. Lett.*, **490**, L1 (1997).

Songaila, A., and Cowie, L. L., *Astron. J.*, **112**, 335 (1996).

Tytler, D. *et al.*, in *QSO Absorption Lines*, ed. G. Meylan ed., Springer, p.289 (1995).

Zaldarriaga, M., Spergel, D., and Seljak, U., *Astrophys. J.*, **488**, 1 (1997).